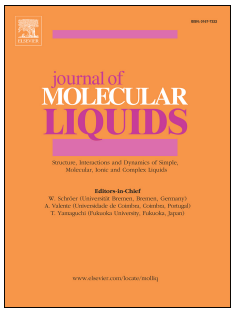

New chemical-physical properties of water after iterative procedure using hydrophilic polymers: The case of paper filter

Vittorio Elia, Elena Napoli, Roberto Germano, Rosario Oliva, Valentina Roviello, Marcella Niccoli, Angela Amoresano, Daniele Naviglio, Martina Ciaravolo, Marco Trifuoggi, Tamar A. Yinnon

PII: S0167-7322(19)34213-8

DOI: https://doi.org/10.1016/j.molliq.2019.111808

Reference: MOLLIQ 111808

To appear in: *Journal of Molecular Liquids*

Received Date: 27 July 2019

Revised Date: 21 September 2019

Accepted Date: 23 September 2019

Please cite this article as: V. Elia, E. Napoli, R. Germano, R. Oliva, V. Roviello, M. Niccoli, A. Amoresano, D. Naviglio, M. Ciaravolo, M. Trifuoggi, T.A. Yinnon, New chemical-physical properties of water after iterative procedure using hydrophilic polymers: The case of paper filter, *Journal of Molecular Liquids* (2019), doi: https://doi.org/10.1016/j.molliq.2019.111808.

NEW CHEMICAL-PHYSICAL PROPERTIES OF WATER AFTER ITERATIVE PROCEDURE USING HYDROPHILIC POLYMERS: THE CASE OF PAPER FILTER.

Vittorio Elia[1], Elena Napoli[1], Roberto Germano[2], Rosario Oliva[1], Valentina Roviello[3], Marcella Niccoli[1], Angela Amoresano[1], Daniele Naviglio[1], Martina Ciaravolo[1], Marco Trifuoggi[4], Tamar A. Yinnon[5]

[1] Department of Chemical Sciences, University "Federico II", Complesso Universitario di Monte Sant'Angelo, Via Cintia, I-80126 Napoli, Italy.
[2] PROMETE Srl, CNR Spin off, P.le V. Tecchio, 45 I – 80125 Napoli, Italy.
[3] Advanced Metrologic Service Center (CeSMA), University of Napoli "Federico II", Corso Nicolangelo Protopisani, 80146 - Napoli, Italy
[4] Analytical Chemistry for Environment Institute of the Chemical Science Department of the "Federico II" University of Napoli, Italy.
[5] K. Kalia, D.N. Kikar Jordan, 90666, Israel.

[*]Corresponding author e-mail: germano@promete.it

Abstract

It is taken for granted that paper filters (inert cellulose filters) do not affect water. However, our experiments show that after such filters repeatedly touched water, the liquid is modified. For example, the liquid's electric conductivity, density, structure and composition are modified. The modifications neither are ascribable to impurities present in the filter nor to organic- or biological pollutants. Our data show that the filters instigate association of water molecules and produce organic molecules. Seemingly, the water-filter interface catalyses reactions involving atmospheric molecules. Our findings may have implications for procedures wherein water repeatedly touches cellulose filters.

Keywords: Water, paper filter, cellulose, interfacial water.

1. Introduction

As a matter of course, it is presumed that cellulose paper filters (PF) do not affect aqueous systems. PF are inert, hydrophilic, in water insoluble polymers (1). However, our experimental data led us to doubt this presumption. We have shown that Milli-Q® water repeatedly touching other varieties of inert insoluble cellulose modify many of its physicochemical properties (2-5). For example, it modifies the liquid's electric

conductivity (χ), density, heat of mixing with base, pH, structure and spectra [ultraviolet (UV), visible (vis), infra-red (IR), circular dichroism spectra] (CD) (2-5) and Fluorescence spectra.

The modifications are not ascribable to impurities present in the cellulose or to other pollutants, as our advanced analytical techniques show (2-5). Instead, our experimental data hint that on submerging cellulose in water, interfacial water stabilizes. When subsequently we gently splash the liquid against the cellulose, clomps of interfacial water loosen and diffuse into the bulk liquid (2, 5).

The goal of our current study is to investigate the effects of water repeatedly touching PF. Such a study is significant, because PF is ordinarily used in many laboratories.

2. Results

2.1 Samples and controls

2.1.1 Samples

We let Milli-Q® water repeatedly touch PF in the same manner as we did for cellophane strips, which is described in Ref. 5. In summary, we washed a PF in Milli-Q® water and dried it in air. After that, we repeated tens of times the following procedure: submerging a dried PF in Milli-Q® water held in an open polystyrene Petri dish, gently stirring the liquid, measuring its χ, reshuffling the PF, 10-50 times repeating the afore mentioned steps, removing the PF and drying it in air. The variation depends not only on the number of iterations, but also on the volume of the sample and the time of hydration; for this reason we speak of a range (10-50 times) and not of an exact number. We term the water in the dish, after the PF was taken out, "iteratively perturbed water (IPW)". In our previous articles, we termed water after it has repeatedly touched cellophane (CE) as IPW-CE. Accordingly, we term water that has repeatedly touched PF as IPW-PF. Production of water repeatedly perturbed with hydrophilic cellulose, Paper filters (PF) and Hydrophilic Cotton, (HC), *i.e.*, IPW-PF (PF) and.IPW-HC , is nearly the same as that of IPW-CE (2). The differences are that the water is not stirred and that after the HC or PF has been pulled out of the water they are squeezed.

We typify IPW samples by their χ (χ_{IPW}). Measuring χ is simple and does not destruct or pollute specimen. Each reshuffle of the polymer enhances χ. The enhancements surpass the experimental error after several shuffles. χ_{IPW} varies with the number of polymer submersion-extraction cycles, the amount of water in the dish, the surface

area of the polymer, shifts in ambient parameters and storage. On storing samples for periods of several days, months or years, their χ_{IPW} may initially grow and then drop, or first lessen and then rise, always grow or constantly drop (for IPW-PF see Fig. 1, for IPW-HC see fig. S1 in Ref. 2). The storing and volume dependencies are characteristic of out-of-equilibrium, auto-organizing, dissipative liquids.

Measurements and alternating ambient conditions affect these properties. Despite these limitations, it is possible to reveal specific phenomena (2, 5, and we can reproduce them. For example, we exposed correlations between χ_{IPW}, pH, density and other variables [for IPW-PF see Supplementary Information (SI) fig. S1 and S2; for IPW-CE and IPW-HC see Ref. 2 and 5, respectively]. Aspects of the correlations, like the slope of the linear correlation between the logarithm of χ_{IPW} and the pH, are sensitive to the composition of the perturbing polymer (5). The correlations imply that IPW have fractal properties assignable to coherent dynamics (see Section S6 of Ref. 2 and Ref. 6 and references therein). In regard of the afore mentioned, we report properties for several specimen with varying χ_{IPW}.

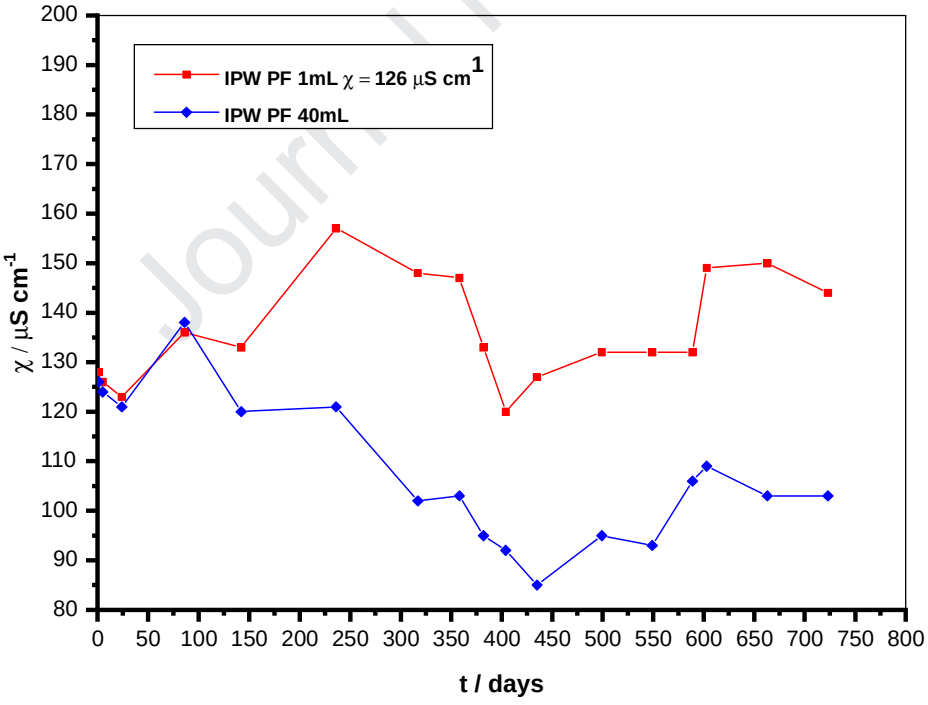

Fig. 1. Graphic of the electrical conductivity χ of two identical aging IPW-PF specimen of different volume. The specimen originated from a sample that was divided in two parts, *i.e.*, the specimen had the same χ_{IPW} of 126 µS cm^{-1} on the first day of storage [time (t) =1]. The red and blue lines refer, respectively, to a 5 ml and 40 ml specimen kept in polyethylene containers

2.2 Impurity analyses

IPW phenomena are not attributable to impurities (2, 5, 7-12). The results of our impurity analyses of IPW-PF, which are similar as those we obtained for the other varieties of IPW (2, 5, 7-12), are as follows:

- Although, initially the growth of χ_{IPW} with each shuffle of the polymeric strip could be due to solvation of its ionic impurities, ultimately the number of dissolving ions should diminish exponentially. Thus, such ions cannot cause the growth in χ_{IPW} after many reshuffles (2, 5, 12).
- Producing IPW with new polymeric strips or many reuses of old ones does not impact on IPW phenomena (2, 5, 12).
- Pollution by the experimentalist is incommensurate with the facts that during production of IPWs, the pH of IPW-PF does not change, the pH of IPW-CE or IPW-HC reaches values up to ~8-9 while that of IPW-N drops to ~3 (2, 5, 11).
- χ_{IPW} may grow by a factor of about 10^3-10^4 (2, 5, 11), *e.g.*, up to ~1480 micro Siemens per centimeter (μS cm^{-1}) for IPW-PF (see SI Table S2). χ of Milli-Q® water is about 1 – 2 μS cm^{-1}. Addition of several grams of electrolytes to a liter of water is needed to let its χ grow by the afore cited factor. The washed, inert polymeric strips, employed for producing the various IPWs, do not add such quantities of ionic impurities. Ion Chromatography (IC) of IPW-PF and all other IPW varieties has confirmed that their electrolytes' mass is less than the detection-limit (~10^{-1} milligram per gram) (2, 5, 11).
- The ups, downs and re-ups in χ_{IPW} observed during storage of samples, *e.g.*, see Fig. 1, are not assignable to impurities (2, 5, 11). The concentration of impurities does not grow, go down and regrow and so forth.
- Some additional data of IPWs are incommensurate with these being due to impurities - see sections 2.3.1 and 2.4.

2.3 Physicochemical data

2.3.1 Titrations

Conductometric titrations show that some reagent, which reacts with hydrochloric acid (HCl) as a weak base with a strong acid, is present in IPW-PF (see Fig. 2) and in other IPW varieties (2, 5). The conductometric titrations were performed measuring

the specific electrical conductivity of a solution of PF (1-3 mL) as a function of the volume of added HCl, and thus of the concentration of the added probe in the final solution (the molarity of HCl indicated with M^{f}_{HCl} / mol L^{-1}).

The curve of the conductivity titration shows an equivalent point, which is determined by the intersection of the two straight lines. The equivalent point varies with the specimen's χ_{IPW} and indicates that it contains ~10^{-4} mol/l of the reagent.

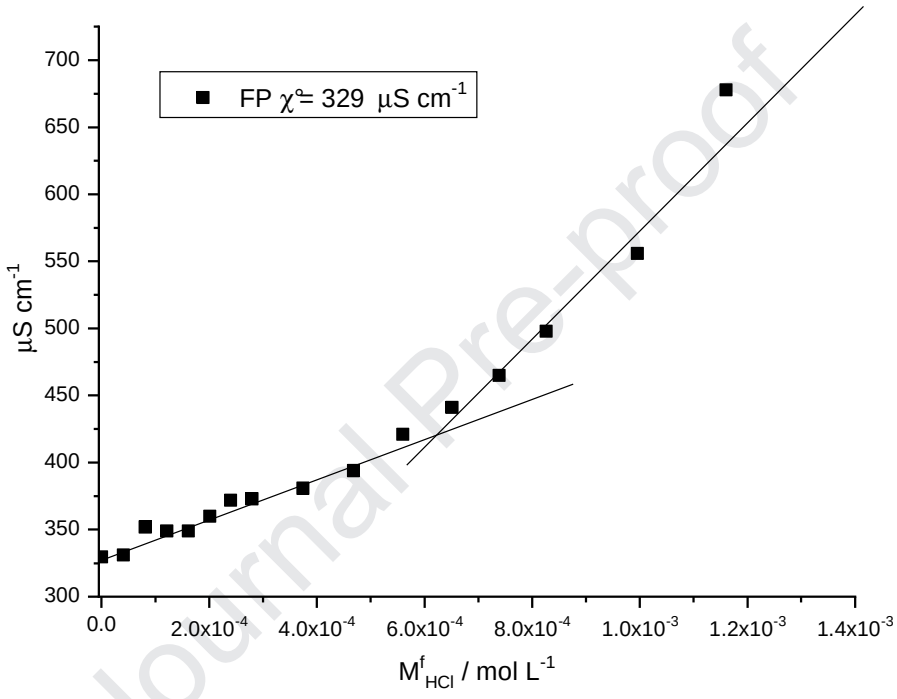

Fig. 2 - Conductometric titration of an IPW-PF sample with HCl. χ as a function of the concentration of HCl in the final solution (M^{f}_{HCl} mol/l). χ of the sample before the start of the titrations (χ^{o}) is 329 µS cm^{-1}.

Calorimetric titrations show that the reagent interacts with sodium hydroxide (NaOH). Fig. 3 displays the excess enthalpy of mixing ΔH^{E} (see Method Section 5) as a function of the concentration m^{f}_{NaOH} (mol/l) of NaOH in a titrated IPW-PF specimen. The figure is typifying for all IPW varieties and signifies that the reagent and the titrate form a complex (2, 5, 13-15). ΔH^{E} obtained on adding HCl to IPW is too low to obtain significant titration data.

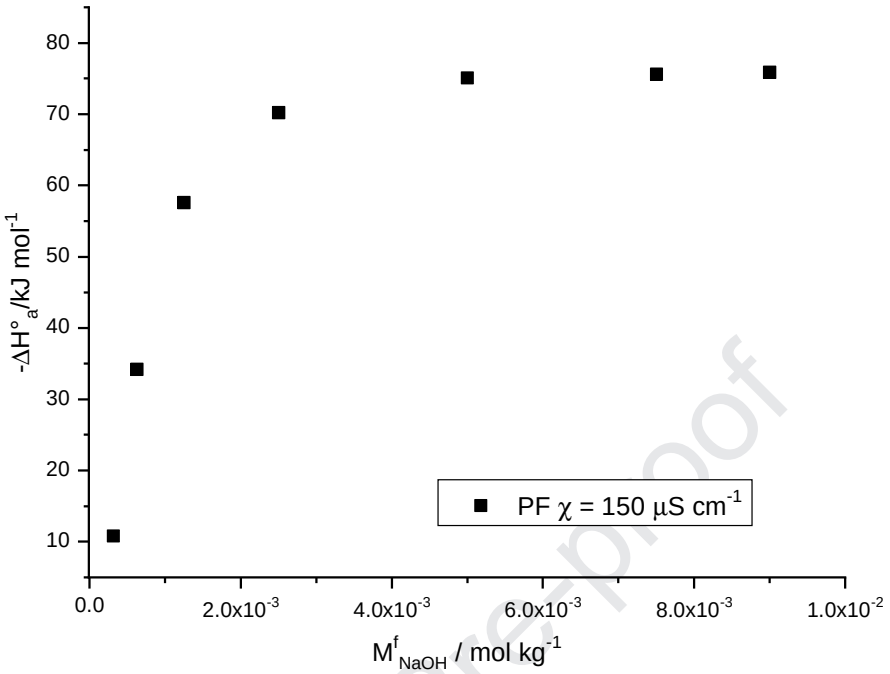

Fig. 3 - $-\Delta H^E$ as function of M^f_{NaOH} / mol/l in a titrated IPW-PF specimen. χ_{IPW} of the specimen before the titration was 150 µS cm^{-1}.

The concentration of m_{PF}, in mol L^{-1}, is obtained via conductometric titration. This value is obtained from the experimentally determined equivalent point, $M_{e.p.}$ / mol L^{-1}, obtained in the conductometric titration.

For the calculation of thermodynamic quantities that characterize the binding process, the ΔH^E is normalized for the concentration determined by conductometric titration. ΔH^E and other thermodynamic variables of the mixing process (the standard free energy and entropy) contain information on the interactions between the titrant and the reagent. Table 1 presents the values of these variables for several IPW-PF samples.

Table 1 – Thermodynamic parameters for the association between the entities present in IPW-PF and OH^- ions at 298 K

System	χ_{IPW}^{i} µS cm^{-1}	*n*	K'_a	$-\Delta H°_a$ kJ/mol	$-\Delta G°'_a$ kJ/mol	$T\Delta S°'_a$ kJ/mol
IPW-PF	150	1	2689±489	80±2	19.6±0.5	-60±2

χ_{IPW}^{i} is the electric conductivity of the samples before the start of the titration. *n*, K'_a ,$-\Delta H°_a$, $-\Delta G°'_a$ and $\Delta S°'_a$ are defined in Section 5.3 in Ref. 2. *n* is the binding stoichiometry. K'_a represents the apparent association constant. $-\Delta H°_a$ represents the standard molar enthalpy of association. $-\Delta G°'_a$ represents the standard free energy. $\Delta S°'_a$ represents the standard entropy. *T* represents the temperature in degrees Kelvin (K). The reported errors are the standard deviations as obtained by fitting the data to Eq. 5 in Section 5.3 in Ref. 2. Errors are half the range of $\Delta G°'_a$ calculated from the upper and lower error in K'_a. Errors are the sum of the errors on free energy and enthalpy.

Calorimetric measurements of the dilution enthalpy were performed on the PF samples. Heats of dilution of PF in water have been determined at 298.15 K by flow microcalorimetry. From these measures it was possible to determine the enthalpic coefficient of interaction (see Method Section 5). These coefficients are derived as pairwise coefficients of the virial expansion of the excess thermodynamic properties of a solution. The enthalpic coefficients give information on how two hydrated molecules interact with each other in solution, and about the forces ruling that process. The physical meaning of coefficients is linked to experimented variations in thermodynamic properties during the dilution process. The analysis of the enthalpic coefficients give information about the intermolecular interaction mechanism and the various contributions acting in the interaction.

The h_{xx} values for PF samples are high and positive Fig. 4. According to the proposed phenomenological classification for non-electrolytes [ref W.G. McMillan Jr. and E. Mayer: J. Chem. Phys. 13, 276 (1945). J.J. Kozak, W.S. Knight, and W. Kauzmann: J. Chem. Phys. 48, 675 (1948). H.L. Friedman and V. Krishnan: J. Solution Chem. 2, 119 (1973).], PF samples can be considered as hydrophobic structure makers (g_{xx} >0, h_{xx} >0 and Ts_{xx}<0)

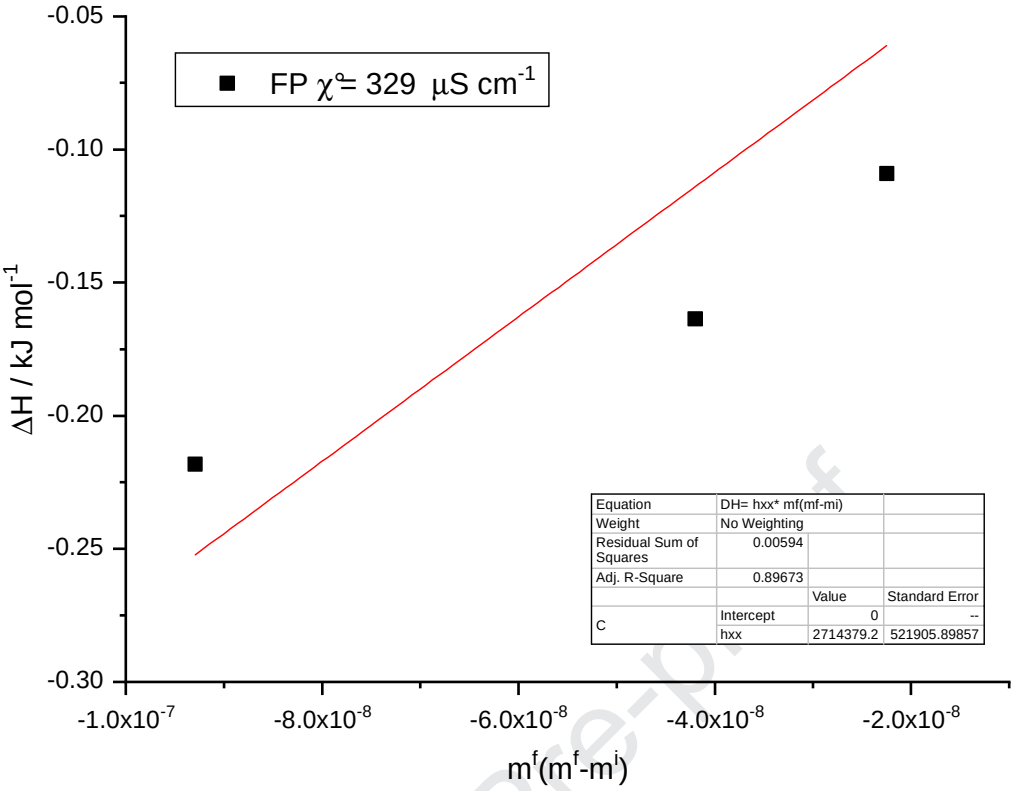

Fig. 4 - It is here shown how the h_{xx} values for PF samples are high and positive, according to the proposed phenomenological classification for non-electrolytes. The line has to intercept zero, too, because at zero, also the DH is zero; but, we represent the line in this range to visualize it better.

An impurity-based explanation of the titration data is easy to dismiss - see Section 2.2. Moreover, the data resemble those we obtained for water repeatedly filtered through cellulose nitrate filters (IPW-F_{CN}) (3).

2.3.2 Spectra

The UV absorbance, fluorescence and circular dichroism (CD) spectra of IPW-PF resemble those of all other IPW varieties. The spectra of the latter were reported in Refs. 1, 4, 5, 7 and 11. The UV absorbance and fluorescence features of IPW are typifying for supramolecular ordered waters, *e.g.*, aqueous solutions, water bordering on hydrophilic materials (16 - 20). These liquids absorb radiation with 200 - 350 nm wavelength. In contrast, water vapour, bulk water at 25°C and 1 atm., amorphous, hexagonal or cubic ice do not significantly absorb 200 – 350 nm radiation (21, 22). Associates of water (H_2O) molecules seem to absorb the 200 - 350 nm radiation (2, 11, 12, 20, 23). Such absorbance has been predicted by the widely used, *ab initio* derived, Complete-Active-Space Self-Consistent-Field Second-order Perturbation

Theory (CASPT2) (20, 23). Moreover, it conforms to predictions of quantum physics when long-range dispersion interactions are explicitly described (2, 11, 12, 24, 25).

Fig. 5 presents the fluorescence spectra of an IPW-PF specimen and of Milli-Q® water. The wavelength of the excitation radiation was 280 nm. The two bands in the spectrum of IWP-PF do not appear in that of Milli-Q® water. The latter only exhibits a very small peak at 310 nm due to Raman scattering by H_2O molecules (26). The high intensity of the fluorescence of IPW-PF blurs its Raman scattering, as is also the case for IPW-HC (2). The spectrum of IPW-PF resembles that of IPW-HC and IPW-CE - see Fig. 3, Fig. 3A in Ref. 2 and Fig. 15 in Ref. 5. The featureless, very broad fluorescence bands of IPW hint that it contains excimers (2, 5, 20, 23).

The impact of radiation on IPW-PF is not just distinguishable with spectroscopy. It is visible: just as all other IPW varieties, IPW-PF has a pallid-yellow tint – see Fig. 4. The tint intensifies when χ_{IPW} grows. Fig. 6 also shows that although IPW-PF is a transparent liquid, it contains some dust like material. In contrast, IPW-HC and IPW-N just consist of fully transparent liquids. IPW-CE is a turbid liquid, but it does not contain solid material – see Fig. 17 in Ref 5.

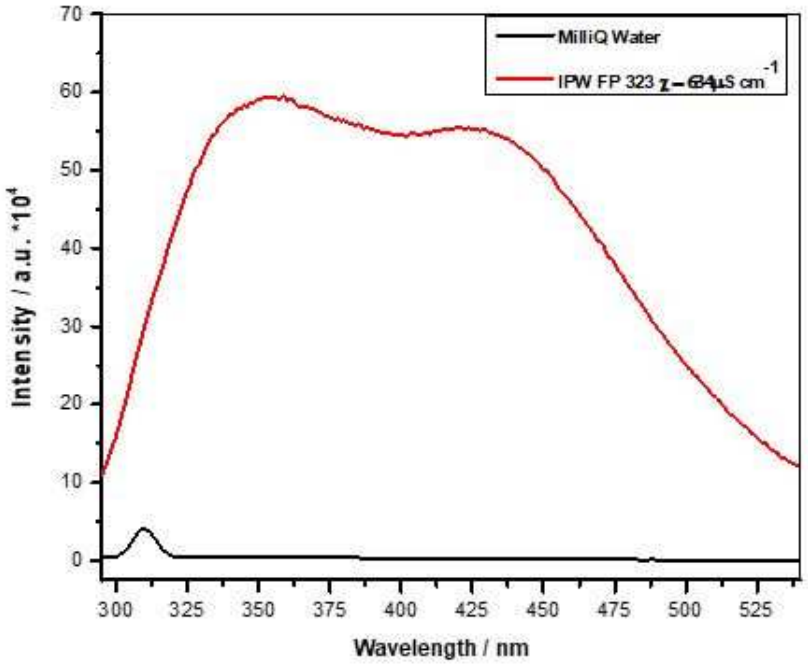

Fig. 5 - Fluorescence spectra. The spectra of an IPW-PF specimen with χ_{IPW} = 323 µS $cm^{-1}$and of Milli-Q® water. The specifications of the specimen are noted in the inset. The liquids were kept at 25 ^{o}C. The bandwidths of both the excitation and emission monochromator were 5 nm. The fluorescence intensity is presented in arbitrary units (a.u.).

Fig. 6 - An IPW-PF sample in its liquid state. Something seems to go out the liquid phase.

IPW-PF is optical active, as its CD spectrum displayed in fig. S3 shows. The figure also shows that Milli-Q® water is optical inactive, because H_2O molecules are achiral. The CD spectrum of IPW-PF resembles those of the other types of IPW (compare fig. S3 with: Fig. 2 in Ref. 2, Fig. 14 in Ref. 5, Figs. 4 and 6 in Ref. 11). The CD spectra of all IPW varieties have the typifying features present in the CD spectra of β-sheet ordered biological molecules (27). The CD of IPW means that it contains chiral entities. Hydrogen bonds among H_2O molecules are not critical for sustaining the chirality of the entities. Mixing IPW with NaOH until its pH rose to 13 does not destroy its optical activity. Moreover, mixing IPW with HCl or Guanidinium Chloride until its pH dropped to 3 does not extinguish its optical activity (2, 5, 11).

2.4 Properties of the entities present in IPW

The entities in IPW are isolatable by removing bulk H_2O molecules by lyophilization. ~20 mg of residue (R_{IPW}) is obtained on lyophilizing ~100 ml of IPW. The R_{IPW} of IPW-PF ($R_{IPW\text{-}PF}$) is a chunky solid - see Fig. 7, that of IPW-CE ($R_{IPW\text{-}CE}$) is a jelly-like polymer (5), that of IPW-N ($R_{IPW\text{-}N}$) is a network-like solid of pale brown color (11), while that of IPW-HC ($R_{IPW\text{-}HC}$) is a powder (2).

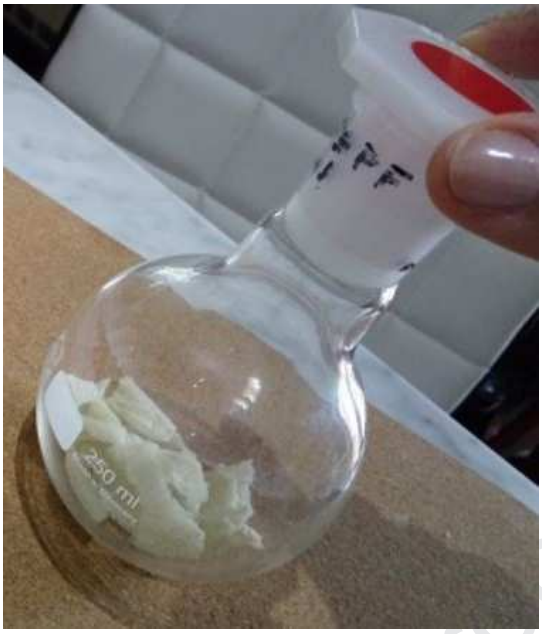

Fig. 7 -The chunks left over after lyophilizing IPW-PF.

R_{IPW} is stable up to high temperatures (*T*). Thermogravimetry (TG) shows that on heating R_{IPW-PF} up to 950^{o}C (at ~1 atm.) part of it perseveres– see Fig. 8. Fig. 8A presents TG results for R_{IPW-PF} specimen that were obtained by lyophilizing IPW-PF either in an oxidizing environment (air) or in an inert gas (nitrogen - N_2), and subsequently heated, respectively, in air or N_2. We denote the former specimen as $R_{IPW-PF-air}$ and the latter as $R_{IPW-PF-N2}$. The TG lines of $R_{IPW-PF-air}$ and $R_{IPW-PF-N2}$ are about identical for *T*<~250^{o}C, but these diverge at higher *T*. For *T*>~ 400^{o}C, the former has more points of inflection than that of the latter. This implies that $R_{IPW-PF-}$ contains ingredients sensible to oxidation

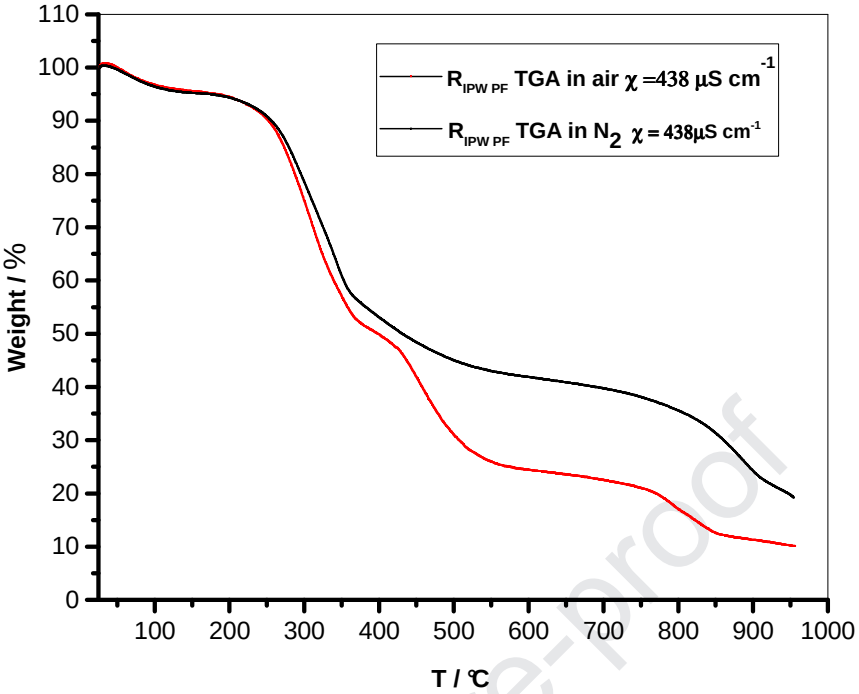

277 **A**

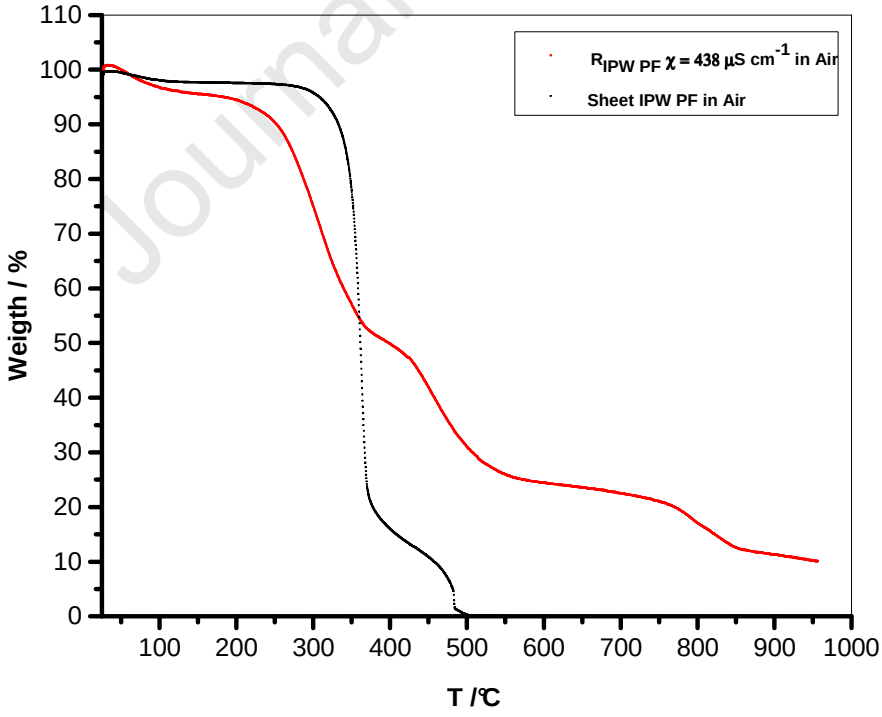

278

279 **B**

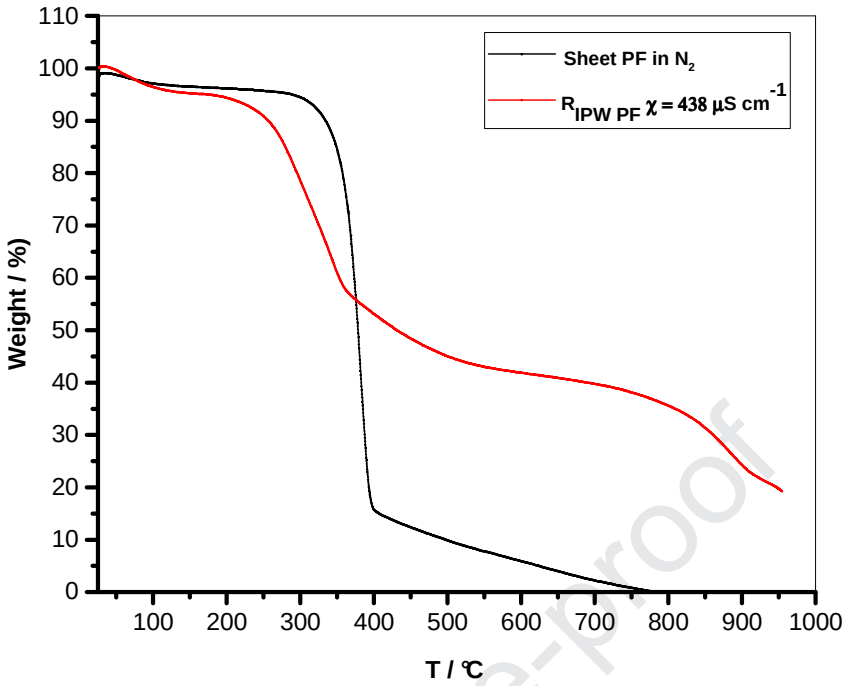

C

Fig. 8 – Thermogravimetry at ~1 atm. (A) TG lines of $R_{IPW\text{-}PF\text{-}air}$ and $R_{IPW\text{-}PF\text{-}N2}$. (B) TG lines of $R_{IPW\text{-}PF\text{-}air}$ and PF in air. (C) TG lines of $R_{IPW\text{-}PF\text{-}N2}$ and PF in N_2. The lines show the diminishments in weight (%) of the specimen due to their heating up to specific temperatures (in ºC). The $\chi_{IPW\text{-}PF}$ of the IPW-PF from which $R_{IPW\text{-}PF}$ was prepared was 438 µS cm^{-1}.

The TG lines of $R_{IPW\text{-}PF\text{-}N2}$ and $R_{IPW\text{-}PF\text{-}air}$ noticeably deviate from those of PF heated in, respectively, N_2 or in air – see Fig. 8B&C. The TG lines of PF are typifying for cellulose (28). The deviations support our previous conclusions that the properties of IPW-PF are not assignable to impurities originating in the PF (see section 2.2). The deviations also imply that these properties are not due to traces of PF. The deviations signify that the chemical make-up of $R_{IPW\text{-}PF}$ and that of PF is different, *i.e.*, some chemicals are produced during the repeated interaction between water and PF. Indeed, our elementary analyses show that $R_{IPW\text{-}PF}$ is much richer in oxygen (O), poorer in carbon (C) and hydrogen (H) atoms than PF – see Table 2.

Table 2 – Percentage in weight of the elements C, H and O in $R_{IPW\text{-}PF\text{-}air}$ and in PFin air.

Elements	*C*	*H*	*O*
$R_{IPW\text{-}PF\text{-}air}$	11,3	2,7	86,0
PF	51,1	8,84	40,0

The TG curves of $R_{IPW\text{-}PF\text{-}air}$ and $R_{IPW\text{-}PF\text{-}N_2}$ both look like their counterparts of $R_{IPW\text{-}CE}$ ($R_{IPW\text{-}CE\text{-}air}$ and $R_{IPW\text{-}CE\text{-}N_2}$) - compare Fig. 8A and Ref. 2's Fig. 12B. Moreover, just as the TG lines of $R_{IPW\text{-}PF}$ noticeably deviate from those of PF, the TG lines of $R_{IPW\text{-}CE}$ markedly differ from those of CE strips (see Ref. 2's Fig. 12A). Thus, both during the repeated interaction of water with PF or with CE strips, chemical reactions take place. The TG lines of $R_{IPW\text{-}PF\text{-}air}$ and $R_{IPW\text{-}CE\text{-}air}$ have some meaningful resemblances with those of $R_{IPW\text{-}N\text{-}air}$ (the residue of IPW-N lyophilized and subsequently heated in air) – compare Fig. 8A with Ref. 12's Fig. 3.

$R_{IPW\text{-}PF}$ contains molecules with 100-1000 masses per unit charge (*m*/*z*), as the mass-spectroscopic data with MALDI-TOF as ionization technique show – see Table. S1. $R_{IPW\text{-}CE}$ also contains such molecules (5). In $R_{IPW\text{-}N}$ or $R_{IPW\text{-}HC}$, no such molecules are observable with MALDI-TOF, gas chromatography or Gel electrophoresis (2, 11). [Observation of molecules with the afore mentioned techniques requires that their concentration is above, respectively 0.1 pmol/µl, 0.5 pmol/µl or 0.25 ng/band for Coomassie stain (GelCode Blue Stain Reagent, Product # 24592).] Currently, we investigate the characteristics and origin of the molecules with the high m/z values.

3. Discussion

Our experiments show that after Milli-Q® water repeatedly touched PF, it is modified. In summary: Most of the modifications resemble those of Milli-Q® water after it repeatedly touched other hydrophilic materials (cellophane, cotton wool, cellulose nitrate, Nafion). (The data concern the water left in the dish after the material has been taken out.) The modifications cannot be ascribed to pollutants. Instead, during the repeated contact, 10^{-4}-10^{-3} mol/l of chiral entities composed of excimers are created, as conductometry, calorimetry, UV absorbance, emission and circular dichroism spectra show. The entities cause the density and χ of the perturbed waters to be

significantly higher than those of Milli-Q® water. The length of the entities may reach 10^{-4} m, as visualized by optical-, fluorescence-, atomic force- and scanning electron-microscopy of Milli-Q water perturbed by cellophane, cotton wool, cellulose nitrate or Nafion (2, 4, 5, 7, 10, 11). The entities are isolatable by lyophilization. TG shows that the entities contain associates of H_2O molecules. Moreover, for water perturbed by PF or cellophane, the entities contain significant amounts (up to 50%) of organic molecules, as TG, MALDI-TOF and elementary analyses show. The chemical compositions of the entities significantly differ from that of the perturbing materials.

A possible explanation for formation of the entities is the following (2, 5, 11, 12): Firstly, when we submerge hydrophilic materials in Milli-Q® water, H_2O molecules associate at their interface. The associates are chiral. Generally, physisorbed achiral molecules form chiral super-structures (33).[1] Secondly, the interface catalyzes chemical reactions involving atmospheric molecules. At interfaces like bubbles, vessel walls or hard micro-impurities, such molecules may react with dissociated H_2O molecules (36). Carotenoids, amides, esters or sugars have been identified in ultra-pure water flowing through acrylic resin micro-orifices (37, 38). Thirdly, when we shuffle the submerged materials, clomps of interfacial liquid loosen and diffuse in the liquid. At hydrophilic materials, interfacial water may reach out up to distances of 10^{-4} m (18, 19, 39, 40). Such water excludes relatively large molecules, like pH-indicators, biological molecules, cells or colloid suspensions. Accordingly, it has been denoted "Exclusion Zone" (EZ) water (18). It easily loosens - it can spontaneously separate from the interface (41). In support of this explanation we note that EZ water shares several properties with water perturbed by hydrophilic materials (12). For example, their UV absorbance-fluorescence spectral features are similar (see section 2.3.2 and Refs. 2, 5, 11, 18 - 20), their densities are higher than that of bulk water (see Fig. S2 and Refs. 2, 5, 12),[2] both exhibit chiral symmetry-breaking phenomena (see section

[1] In 2017, H_2O molecules adjacent to DNA - in an almost physiological environment - were observed to organize chirally (34). Measurements carried out before publication of these observations, which were undertaken to distinguish between the H_2O hydration molecules of DNA and those of bulk water, were not pertinent to such hydration in biological environments. We did not find any explanations in the literature for this 2017 observation. We opinion that the observation signifies for DNA our optical activity data of water perturbed by hydrophilic materials (35).

[2] The density of the EZ water of Nafion is ~17 percent higher than that of bulk water at 25 ^{o}C and 1 atm. (40). The density of EZ water at cellulose interfaces, to the best of our knowledge, has not yet been measured.

2.3.2 and Refs. 2,5, 11, 42) and the maximal breadth of the EZ and the length of the entities in IPW are of the same order.

5. Conclusions

Our data overturn the usual assumption that paper filter does not affect the chemistry of water. Our findings are significant for technological processes, which are sensitive to the electric conductivity, density, structure, chemical composition and optical activity of water.

5. Materials and Methods

The PF used for preparing IPW-PF are about 50 filters of circular shape of 12 cm diameter by Carlo Erba (code: 289200123). We determined the presence of inorganic molecules in the PF in the same manner as we did for cellophane, which is described in Ref. 5.

The experimental design and the following methods are exactly as those described in Ref. 2: electric conductivity, pH, Ion Chromatography (IC), density, MALDI-TOF coupled with MS, UV absorbance and fluorescence, CD, calorimetry (including the definition of the excess enthalpy of mixing ΔH^{E}) measurements. The following methods are exactly the same as detailed in Ref. 5: lyophilization and thermogravimetry. The Elementary analyses were performed as detailed in Ref. 2.

Supplementary

Figure S1 - pH of IPW-PF samples as function of χ_{IPW}

Figure S2 - The logarithm of the density of IPW-PF as a function of the logarithm of its χ_{IPW}

Figure S3 – Circular dichroism spectra.

Table S1 – MALDI-TOF/MS

Table S2 - Conductivity $\chi_{IPW\text{-}PF}$ and pH of IPW-PF samples

Acknowledgments

Tamar Yinnon thanks Prof. A.M. Yinnon for his support.

Author contributions

V.E. . planned and directed the research. RG assisted in the latter task, E.N. produced the perturbed waters. R.O. carried out the spectral measurements. A.A. carried out the MALDI-TOF/MS measurements. E.N. measured the electric conductivity, pH. and density, M.N. performed thermodynamic analyses. M.T.. carried out the Elemental analyses of the incinerated PF and of RIPW-PF. V.R. contributed to the thermogravimetric analyses. D.N. and M.C. made lyophilization procedures and managed the analytic chemistry measurements, T.A.Y. wrote the manuscript. The findings and the manuscript were debated by all coauthors.

Competing interests

The authors declare no competing financial interest.

References

1. D. Klemm, B. Heublein, H.P. Fink, A. Bohn, Cellulose: Fascinating biopolymer and sustainable raw material. *Angew. Chem. Int. Ed*. **44**, 3358–3393 (2005).
2. V. Elia, R. Oliva, E. Napoli, R. Germano, G. Pinto, L. Lista, M. Niccoli, D. Toso, G. Vitiello, M. Trifuoggi, A. Giarra, T. A. Yinnon, Experimental study of physicochemical changes in water by iterative contact with hydrophilic polymers: A comparison between Cellulose and Nafion**.** *J. Mol. Liq*. **268**, 598–609 (2018).
3. V. Elia, N. Marchettini, E. Napoli, M. Niccoli, Calorimetric, conductometric and density measurements of iteratively filtered water using 450, 200, 100 and 25 nm Millipore filters. *J. Therm. Anal. Cal*. **114**, 927–936 (2013).
4. V. Elia, G. Ausanio, A. De Ninno, R. Germano, E. Napoli, M. Niccoli, Experimental evidences of stable water nanostructures at standard pressure and temperature obtained by iterative filtration**.** *Water* **5**, 121-130 (2014).
5. V. Elia, Water perturbed by Cellophane: Comparison of its physicochemical properties with those of water perturbed with cotton wool or Nafion. submitted.to JTAC
6. A. Capolupo, E. Del Giudice, V. Elia, R. Germano, E. Napoli, M. Niccoli, A. Tedeschi, G. Vitiello, Self-similarity properties of Nafionized and

filtered water and deformed coherent states. *Int. J. Mod. Phys. B* **28**, 1450007 (2014).

7. V. Elia, G. Ausanio, A. De Ninno, F. Gentile, R. Germano, E. Napoli, M. Niccoli, Experimental evidence of stable aggregates of water at room temperature and normal pressure after iterative contact with a Nafion® polymer membrane. *Water* **5**, 16-26 (2013).
8. V. Elia, E. Napoli, M. Niccoli, Physical–chemical study of water in contact with a hydrophilic polymer: Nafion, *J. Therm. Anal. Calorim*. **112**, **9**37-944 (2013).
9. V. Elia, L. Lista, E. Napoli, M. Niccoli, A Thermodynamic characterization of aqueous nanostructures of water molecules formed by prolonged contact with the hydrophilic polymer Nafion. *J. Therm. Anal. Calorim*. **115**, 1841-1849 (2014).
10. V. Elia, R. Germano, E. Napoli, Permanent dissipative structures in water: the matrix of life? Experimental evidences and their quantum origin. *Curr. Top. Med. Chem.* **15**, 559-571 (2015).
11. V. Elia, T.A. Yinnon, R. Oliva, E. Napoli, R. Germano, F. Bobba, A. Amoresano, Chiral micron-sized H_2O aggregates in water: Circular dichroism of supramolecular H_2O architectures created by perturbing pure water. *Water* **8**, 1-29 (2017).
12. T.A. Yinnon, V. Elia, E. Napoli, R. Germano, Z-Q Liu, Water ordering induced by interfaces: an experimental and theoretical study. *Water* **7**, 96-128 (2016).
13. V. Elia, M. Niccoli, Thermodynamics of extremely diluted aqueous solutions. *Ann. N. Y. Acad. Sci.* **879**, 241-248 (1999).
14. V. Elia, E. Napoli, Nanostructures of water molecules in iteratively filtered water. *Key Eng. Mate.* **495**, 37-40 (2011).
15. V. Elia, E. Napoli, M. Niccoli, Calorimetric and conductometric titrations of nanostructures of water molecules in iteratively filtered water. *J. Ther, Anal. Calorim*. **111**, 815-821 (2013)
16. S-Y. Lo, Anomalous state of ice. *Mod. Phys. Lett.* **10**, 909-919 (1996).
17. I.S. Ryzhkina, S.Yu. Sergeeva. Y.V. Kiseleva, A.P. Timosheva, O.A. Salakhutdinova, M.D. Shevelev, A.I. Konovalov, Self-organization and

properties of dispersed systems based on dilute aqueous solutions of (S)- and (R)-lysine. *Mendeleev. Commun.* **28**, 66-69 (2018).

18. J.M. Zheng, W.C. Chin, E. Khijniak, E. Khijniak Jr., G.H. Pollack, Surfaces and interfacial water: Evidence that hydrophilic surfaces have long-range impact. *Adv. Colloid Interface Sci.* **127**, 19–27 (2006).
19. B-H Chai, J-M Zheng, Q. Zhao, G. H. Pollack, Spectroscopic studies of solutes in aqueous solution. *J. Phys. Chem. A*, **112**, 2242-2247 (2008).
20. J. Segarra-Martí, P.B. Coto, M. Rubio, D. Roca-Sanjuán, M. Merchán, Towards the understanding at the molecular level of the structured-water absorption and fluorescence spectra: A fingerprint of π-stacked water. *Mol. Phys*. **111**, 1308–1315 (2013).
21. T.I. Quickenden, J.A. Irvin, The ultraviolet absorption spectrum of liquid water. *J. Chem. Phys*. **72**, 4416-4428 (1980).
22. P. Cabral do Couto, D.M. Chipman, Insights into the ultraviolet spectrum of liquid water from model calculations: The different roles of donor and acceptor hydrogen bonds in water pentamers. *J. Chem. Phys.* **137**, 18430 (2012).
23. J. Segarra-Martí, D. Roca-Sanjuán, M. Merchán, Can the hexagonal ice-like model render the spectroscopic fingerprints of structured water? Feedback from quantum-chemical computations. *Entropy*, **16**, 4101-4120 (2014).
24. E. Del Giudice, A. Tedeschi, G. Vitiello, V. Voeikov, Coherent structures in liquid water close to hydrophilic surfaces. *J. Phys.: Conf. Ser*. **442**, 012028 (2013).
25. E. Del Giudice, V. Voeikov, A. Tedeschi, G. Vitiello, The origin and the special role of coherent water in living systems. Chapter 5 in: Fields of the Cell. D. Fels, M. Cifra and F. Scholkman, editors. Research Signpost, Kerala, India (2014).
26. L.V. Belovolova, M. V. Glushkov, E. A. Vinogradov, V. A. Babintsev, V. I. Golovanov, Ultraviolet fluorescence of water and highly diluted aqueous media. *Phys. Wave Phenom*. **17**, 21-31 (2009).
27. G.D. Fasman, Ed., Circular Dichroism and the Conformational Analysis of Biomolecules (Springer Science+Business Media, New York, 1996).

28. W. G. Lee, D. H. Kim, W. C. Jeon, S. K. Kwak, S. J. Kang, S. W. Kang, Facile control of nanoporosity in Cellulose Acetate using Nickel (II) nitrate additive and water pressure treatment for highly efficient battery gel separators. *Sci. Rep*. **7**, 1287 (2017).
29. R. Arani, I. Bono, E. Del Giudice, G. Preparata, QED coherence and the thermodynamics of water. *Int. J. Mod. Phys. B* **9**, 1813-1841 (1995).
30. S. Sivasubramanian, A. Widom and Y.N. Srivastava, The Clausius–Mossotti phase transition inpolar liquids. *Physica A*, **345,** 356 (2005).
31. E. Del Giudice, G. Preparata, G. Vitiello, Water as a free electric dipole laser. *Phys Rev Lett* **61**, 1085-1088 (1988).
32. E. Del Giudice, G. Vitiello, Role of the electromagnetic field in the formation of domains in the process of symmetry-breaking phase transitions. *Phys Rev A* **74**: 022105-1-022105-9.
33. K. H. Ernst, Molecular chirality at surfaces. *Phys. Status Solidi B* **249**, 2057-2088 (2012).
34. M.L. McDermott, H. Vanselous, S.A. Corcelli, P.B. Petersen, DNA's chiral spine of hydration. *ACS. Cent. Sci*.**3**, 708-714 (2017).
35. V. Elia, T.A.Yinnon, R. Oliva, E. Napoli, R. Germano, F. Bobba, A. Amoresano, DNA and the Chiral Water Superstructure. *J. Mol. Liq.* **248**, 1028-1029 (2017).
36. V. Belovolova, E. A. Vinogradov, M. V. Glushkov, Variations in the Water Redox Potential under Ultraviolet Irradiation. *Phys. Wave Phenom*. **21**, 183–189 (2013).
37. T. Hasegawa, A. Ushida, T. Narumi, M. Goda, Is the water flow more or less than that predicted by the Navier-Stokes equation in micro-orifices? *Phys. Fluids*. **28**, 092005, 1-14 (2016).
38. T.Hasegawa, A. Ushida, M. Goda, Y. Ono, Organic compounds generated after the flow of water through micro-orifices: Were they synthesized? Heliyon **3**, e00376 (2017).
39. B. Sulbarán, G. Toriz, G.G. Allan, G.H. Pollack, E. Delgado, The dynamic development of exclusion zones on cellulosic surfaces. *Cellulose* **21**, 1143-1148 (2014).

40. N.F. Bunkin, P.S. Ignatiev, V.A. Kozlov, A.V. Shkirin, S.D. Zakharov, A.A. Zinchenko, Study of the phase states of water close to Nafion interface. *Water* **4**, 129-154 (2013).

41. Y. Zhang, S.Takizawa, J. Lohwacharin, Spontaneous particle separation and salt rejection by hydrophilic membranes. *Water* **7**, 1-18 (2015).

42. X. He, Y. Zhou, X. Wen, A.A. Shpilman, Q. Ren, Effect of Spin Polarization on the Exclusion Zone of Water. *J. Phys. Chem. B* **122**, 8493–8502 (2018)

Supplementary Materials

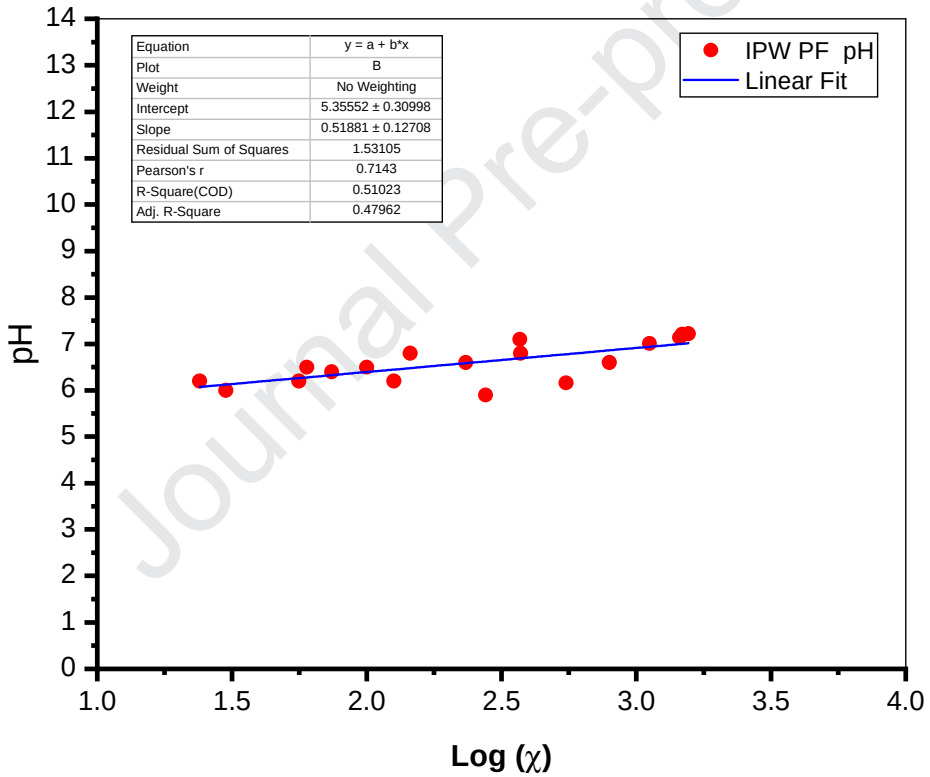

Fig. S1 - pH of IPW-PF samples as function of the logarithm of their electric conductivity χ. The graph shows that the pH and log (χ) are linearly correlated. The correlation is detailed in the inset.

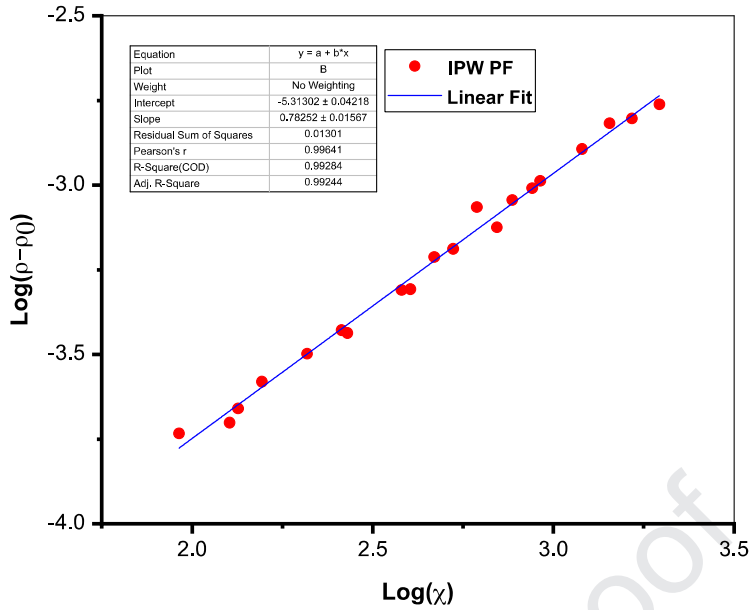

Fig. S2 - The logarithm of the density of IPW-PF as a function of the logarithm of its electric conductivity χ. The linear correlation between the logarithm of the difference between the density of IPW-PF (ρ) and the density of the Milli-Q® water (ρ_0) with which the IPW-PF was prepared, *i.e.*, Log ρ^E = Log (ρ- ρ_0), as a function of the log(χ) of IPW-PF. The correlation is detailed in the inset.

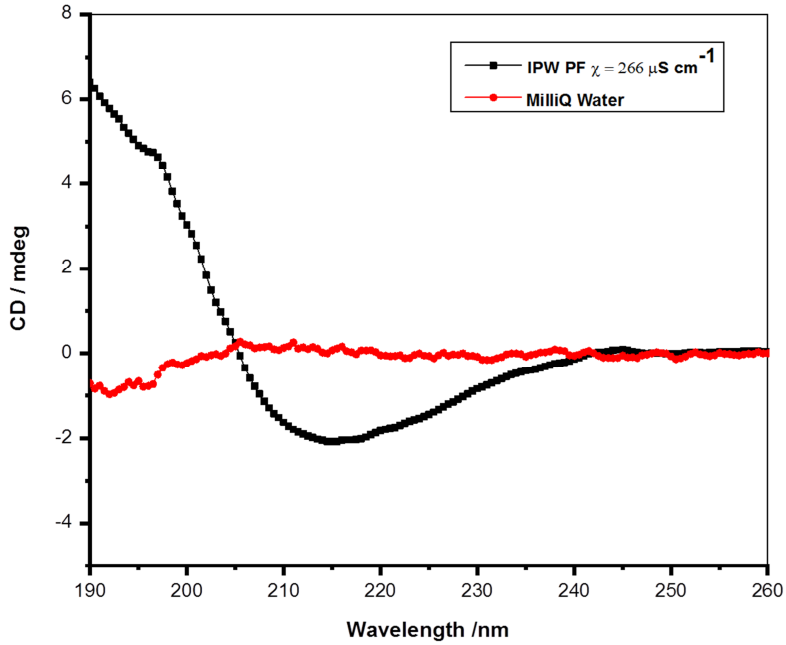

Fig. S3 – Circular dichroism (CD) spectra. The CD in mdeg as a function of the wavelength in nm. The spectra show the difference between the absorbance of left- and right-handed circularly polarized light as a function of the radiation wavelength. The difference is normalized for optical length quartz cuvette (0.5 cm). The spectra are of an IPW-PF sample with χ_{IPW} = 266 µS cm^{-1} and of Milli-Q water. The samples were kept at 25 °C. The sizeable CD values measured for IPW-PF reflect the fact that this liquid is optically active. The negligible CD values measured for Milli-Q water reflect that water is optically inactive, because H_2O is achiral.

PF_t_147 m/z	231	273,1	304,3	362	387,2	501,1	583,1	668,7	750,7	860,8	1160	1460	1587	1876	2057
% Intensity	29	12	12	8	8	4	4	2	2	2	2	2	2	2	2

Table S1 - MALDI-TOF mass spectrum of R_{IPW-PF}. The first line show the mass as the ratio mass / charge (m/z) of the species and the second line show the signal intensity. The limit of detection is around 0.1 pico-mol / µl. This method shows primarily mass signals related to species with a molecular mass ranging from 100 to 1000 m/z.

Table S2 - Conductivity χ_{IPW-PF} and pH of IPW-PF samples

χ_{IPW-PF}	Log(χ_{IPW-PF})	pH	χ_{IPW-PF}	Log(χ_{IPW-PF})	pH
1120	3,0492	7,0	56	1,7482	6,2
1480	3,1703	7,2	126	2,1004	6,2
1450	3,1614	7,1	74	1,8692	6,4
1560	3,1931	7,2	549	2,7396	6,2
24	1,3802	6,2	145	2,1614	6,8
60	1,7782	6,5	233	2,3674	6,6
100	2,0000	6,5	276	2,4409	5,9
370	2,5682	7,1	372	2,5705	6,8
30	1,4771	6,0	795	2,9004	6,6

After that paper filters repeatedly touch pure water, the liquid is modified.

The liquid's electric conductivity, density, structure and composition are modified.

The modifications are not ascribable to impurities.

UV fluorescence spectra of the “perturbed” water cannot be ascribed to contaminants.